Analysis of Rate-Determining Conformational Changes during Self-Splicing of the *Tetrahymena* Intron†

Victoria L. Emerick,‡ Jie Pan, and Sarah A. Woodson*

Department of Chemistry and Biochemistry, University of Maryland, College Park, Maryland 20742-2021

Received April 10, 1996; Revised Manuscript Received June 19, 1996⊗

ABSTRACT: RNA catalyzed reactions are often limited in vitro by the rate of structural rearrangements in the RNA. Analysis of intra- and intermolecular splicing of the *Tetrahymena* preribosomal RNA revealed two well resolved kinetic phases with rate constants of approximately 2.5 and 0.02 min^{-1} at 30 °C. The data are consistent with a model in which the second phase results from slow refolding of the pre-rRNA. Point mutations result in redistribution of the RNA among different conformations that can be detected by native gel electrophoresis. The active pre-rRNA rapidly progresses to a product complex in the presence of GTP. Release of the ligated exons is slightly slower than splicing at 30 °C (0.3 −0.5 min^{-1}). In contrast, the intermediate complex after the first step of splicing dissociates much more slowly (5×10^{-3} min^{-1}), accounting for the low amount of intron-3′ exon intermediate typically seen during splicing of wild type pre-rRNA. These results provide an initial framework for studying conformational changes that accompany excision of the *Tetrahymena* intron from ribosomal RNA.

Conformational flexibility plays a central role in the metabolism and function of many RNAs in the cell. There are many examples in which alternative RNA conformations are the basis for biochemical or genetic regulation (Olender et al., 1979; Chebli et al., 1989; Eng & Warner, 1991; D'Orval et al., 1991; Libri et al., 1991; Dammel & Noller, 1993; Fortner et al., 1994). In other instances, competition between correct and incorrectly folded states can reduce the fraction of native molecules, resulting in reduction or loss of function (Been et al., 1992; Seraphin et al., 1988; Fedor & Uhlenbeck, 1990). A better understanding of the forces that govern formation and stability of RNA structures is important for decoding post-transcriptional regulatory pathways. Moreover, the principles of RNA folding are also a practical concern in the design of therapeutic ribozymes.

Since its discovery, interest in autocatalytic splicing of the *Tetrahymena* intron has centered around the question of how RNA structures are organized such that specific phosphodiester bonds are activated for cleavage (reviewed in Cech & Bass, 1986; Burke, 1988; Cech et al., 1992). The mechanism of group I self-splicing involves binding of GTP (or guanosine) to the precursor RNA, followed by two phosphodiester transesterifications to yield the ligated exon and linear intron RNA products (reviewed in Cech & Bass, 1986). As splice site activation depends on a unique set of RNA interactions, the rate and extent of self-splicing are exquisitely sensitive to the conformational state of the precursor RNA.

Much progress toward understanding cleavage specificity has been made using oligonucleotide substrates that mimic the 5′ and 3′ splice sites (Cech et al., 1992). From work on the riboendonuclease reaction that is catalyzed by the ribozyme form of the *Tetrahymena* intron (Zaug & Cech, 1986), activation of an oligonucleotide substrate that mimics the 5′ splice site occurs in two steps. First, the substrate RNA base pairs with the guide sequence (IGS) to form the P1 helix that contains the 5′ splice site. This RNA helix is then positioned in the active site via non-base pairing interactions (Pyle et al., 1992; Strobel et al., 1995) in a first order process (Bevilacqua et al., 1992; Herschlag, 1992). Binding of the guanosine substrate is also proposed to induce a conformational change in the intron active site (Herschlag & Khosla, 1994; McConnell & Cech, 1995). Recognition of the 3′ splice site in the second step of splicing requires a conserved guanosine at the 3′ end of the intron which must replace the G cofactor in the active site (Been & Perrotta, 1991; Golden & Cech, 1996). Oligonucleotide substrates that mimic the 3′ splice have also provided evidence for a conformational change that is linked to the second step of splicing (Bevilacqua et al., 1996).

Despite these advances, the self-splicing reaction itself remains less well understood. Splicing is more complex than the riboendonuclease reaction in that both cleavage of the 5′ splice site and exon ligation must occur in a coordinated fashion. In addition, *Tetrahymena* precursor RNAs containing natural ribosomal RNA exons (pre-rRNA) can adopt two alternative secondary structures in the 5′ exon, as shown in Figure 1. Besides the active form in which the 5′ exon is base paired with the IGS (P1), a conserved ribosomal hairpin, termed P(−1), can block activation of the 5′ splice site (Woodson & Cech, 1991). The equilibrium between these structures depends on both the primary sequence and length of the exons (Woodson, 1992). It is likely that the relative stabilities of these helices are further modified by non-Watson−Crick interactions within the intron (Pyle et al., 1990) and the ribosomal RNA (Woodson & Emerick, 1993).

The ability of the *Tetrahymena* pre-rRNA to adopt multiple conformations is particularly relevant to the splicing pathway because wild type transcripts are kinetically trapped in a less reactive form when synthesized in vitro at 30 °C (Emerick

† This work was supported by the National Institutes of Health (GM46686). S.W. acknowledges the support of an American Cancer Society Junior Faculty Research Award, the Pew Scholars Program in the Biomedical Sciences, and the Camille and Henry Dreyfus Foundation.

* Author to whom correspondence should be addressed. FAX: 301-405-7956; Phone: 301-405-1836.

‡ Present address: Smith Kline Beecham Pharmaceuticals, 1250 S. Collegeville Rd., UP1345, Collegeville, PA 19426.

⊗ Abstract published in *Advance ACS Abstracts,* September 15, 1996.

S0006-2960(96)00865-3 CCC: $12.00

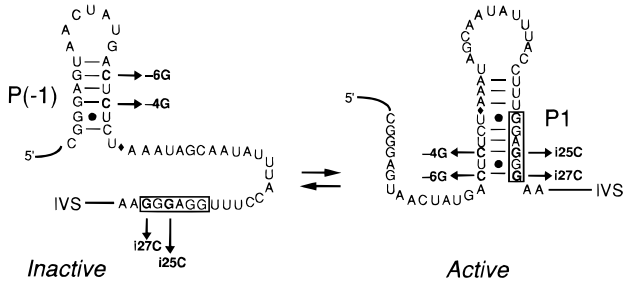

FIGURE 1: Alternative stem-loops in the *Tetrahymena* pre-rRNA. The P1 base pairing between the 5′ exon and the IGS (boxed) is required for 5′ splice site recognition as shown on the right (Been & Cech, 1986). The rRNA P(−1) hairpin on the left competes with P1. Mutations in the 5′ exon (−4 and −6) and in the IGS (i25 and i27) are indicated. Adapted from Woodson and Cech (1991).

& Woodson, 1993). Partially active and fully active forms of the pre-rRNA have been separated by nondenaturing gel electrophoresis (Emerick & Woodson, 1994). The fraction of active form on native gels is increased by thermal renaturation of the RNA, consistent with an increase in splicing activity. Addition of GTP to samples before electrophoresis results in a shift in mobility of the active pre-rRNA. This new band contains both activated pre-rRNA and a complex of intron and ligated exon products (Emerick & Woodson, 1994).

The ability to measure changes in splicing activity along with separation of pre-rRNA conformers on nondenaturing gels provides an opportunity to investigate the conformational changes that accompany intron excision in natural pre-rRNA. To establish a general framework for understanding pre-rRNA splicing, a more detailed investigation of the reaction has been carried out. Kinetic measurements of intra- and intermolecular splicing support a model in which exchange between active and inactive forms of the pre-rRNA is much slower than the rate of transesterification in the presence of near-saturating GTP. A comparison of precursors in which the predicted stability of the alternative secondary structures is modified by sequence changes is consistent with our previous model for 5′ splice site activation in the *Tetrahymena* pre-rRNA (Woodson & Emerick, 1993). Product dissociation is slightly slower than splicing under these conditions, but more rapid than initially predicted from multiple turnover reactions catalyzed by the *Tetrahymena* L-21 ribozyme (Herschlag & Cech, 1990). Less expected is the fact that dissociation of the 5′ exon and the intron-3′ exon intermediates after the first step of splicing is approximately 100-fold slower than release of fully spliced products.

MATERIALS AND METHODS

Preparation of RNA. Plasmid SW012 (Woodson, 1992) encodes a 657 nucleotide precursor RNA derived from *Tetrahymena thermophila* rDNA. Mutated derivatives of pSW012 as shown in Figure 1 were prepared by oligonucleotide-directed mutagenesis (Kunkel et al., 1987). Precursor RNA was transcribed by T7 RNA polymerase from linear pSW012 DNA in the presence of [α-^{32}P]ATP and passed through a TE-100 gel filtration spin column (Clontech) as previously described (Emerick & Woodson, 1993).

Self-Splicing Assays. Reactions containing 0.5−0.7 μM RNA were carried out in splicing buffer (100 mM $(NH_4)_2SO_4$, 50 mM HEPES, pH 7.5, 5 mM $MgCl_2$) at 30 °C and begun with the addition of 0.1 mM GTP as described previously (Emerick & Woodson, 1993). For times between 0 and 12 s, 1.6 μL of buffered RNA solution pre-equilibrated at 30 °C was mixed with 0.4 μL of 0.5 mM GTP on plastic film, and then quenched with the addition of 2 μL of 10 M urea. Data at longer times (15 s−2 h) were collected after addition of GTP to the remaining reaction mixture and removal of 2 μL aliquots at specified times. The two methods produced no detectable disjunction in the resulting progress curves. Reaction mixtures were separated on 4% polyacrylamide gels containing 8 M urea and visualized with a PhosphorImager (Molecular Dynamics).

Where indicated, precursor RNA was heated to 95 °C and cooled in the presence of splicing buffer prior to the start of the splicing assay (Walstrum & Uhlenbeck, 1990; Emerick & Woodson, 1993). In experiments in which the temperature of preincubation was varied, nonrenatured pre-rRNA was incubated in splicing buffer at the indicated temperature for 2 min, placed on ice for 15 s, and then returned to 30 °C for 2 min. Splicing reactions were begun by adding 0.1 mM GTP and carried out at 30 °C for up to 3 min.

Intermolecular (trans) splicing assays for wild type SW012 pre-rRNA were carried out as described above, but without GTP. Instead, reactions were begun with addition of 5′ exon oligonucleotide, $^{5'}$rGGCUCUCU (70 μM final). Trans-splicing oligonucleotide substrates were $^{5'}$rGGGUCUCU for precursors containing the IGS mutation Gi27C and $^{5'}$rGGCUGUCU for Gi25C precursors. Products (5′ exon-IVS and oligonucleotide-3′ exon) were separated on 6% polyacrylamide gels. Ligation of the 5′ exon oligonucleotide to the 3′ exon does not require cleavage of the intramolecular 5′ splice site.

Determination of Kinetic Parameters. The fraction of spliced product (f_{sp}) was determined from the fraction of radioactivity in the ligated exon product for each lane, adjusted for the relative specific activity of the product RNA. Spliced product present at zero time, if any, was subtracted from each data point. The total extent of ligated exon formation at 120 min was typically 80−95%, except for certain mutant pre-rRNAs. Individual time courses were fit to eq 1 using a nonlinear algorithm (KaleidaGraph, Synergy Software, Reading, PA). Reported values for time constants and amplitudes are the average of 2−6 independent isolations of precursor RNA.

Native Gel Electrophoresis and Product Release Assays. Uniformly labeled RNA was prepared as above and separated in 6% polyacrylamide gels containing 34 mM Tris, 66 mM HEPES, 0.1 mM EDTA, and 10 mM $MgCl_2$, pH 7.5, as previously described (Emerick & Woodson, 1994; Pyle et al., 1990). Composition of bands for mutant pre-rRNAs was verified by isolation of RNA from native gels and electrophoresis on 4% denaturing polyacrylamide gels.

To measure dissociation of product complexes, renatured pre-rRNA in splicing buffer plus 10% glycerol and 0.1% xylene cyanol was incubated with 0.1 mM GTP for 1 min or 0.5 mM GTP for 30 s at 30 °C, then shifted to the assay temperature (10−42 °C). Precursor G414A was incubated 2 min with 0.5 mM GTP at 30 °C. At specified times (0−30 min), 5 μL aliquots were loaded on a native 6% gel with the current on. The fraction of product complex (band 3) relative to free product bands (IVS and LE) was calculated based on radioactivity in each lane. The observed rate of dissociation was determined at each temperature from semilogarithmic fits, taking into account the time required for the samples to enter the gel (approximately 30 s).

Dissociation of the intermediate complex was computed in a similar fashion but based on appearance of IVS-3′ exon RNA.

RESULTS

Self-Splicing of Pre-rRNA Is Biphasic. Self-splicing of the *Tetrahymena* intron is expected to follow pseudo-first order kinetics at high concentrations of the G cofactor (Bass & Cech, 1984). Splicing of a 657 nt precursor RNA containing natural rRNA exons, however, does not follow a single exponential curve at physiological temperatures (30 °C) as shown in Figure 2A. Biexponential kinetics suggest the presence of an additional species in the splicing of this pre-rRNA. Since there is no detectable accumulation of intron−3′ exon intermediate and the concentration of GTP (100 μM) is above the apparent K_M for splicing of this precursor (K_M(GTP) = 45 μM; Emerick, 1995), it is unlikely that this additional step involves binding of GTP or exon ligation.

Based on earlier work (Emerick & Woodson, 1993, 1994), a more plausible mechanism for the self-splicing reaction involves exchange between two forms of the precursor, as shown in Scheme 1. For simplicity, it is assumed that both forms of the precursor bind GTP equally and that the rate of reverse splicing is negligible (Woodson & Cech, 1989). Consecutive first order reaction kinetics have been treated by many authors (e.g., Szabó, 1969; Cantor & Schimmel, 1980). The fraction of spliced products, f_{sp}, is described by the equation

$$f_{sp} = A_1(1 - e^{-\lambda_1 t}) + A_2(1 - e^{-\lambda_2 t}) \quad (1)$$

where

$$\lambda_{1,2} = {}^1/_2\{k_1 + k_{-1} + k_2 \pm [(k_1 + k_{-1} + k_2)^2 - 4k_1k_2]^{1/2}\} \quad (2)$$

and $A_1 + A_2 \leq 1$.

Progress curves from self-splicing reactions were fit to eq 1 as shown in Figure 2B, and the results are listed in Table 1. The time constants, λ_1 and λ_2, were found to differ by approximately 100-fold (2.5 min^{-1} vs 0.02 min^{-1}). Renaturation of the pre-rRNA by heating to 95 °C and cooling rapidly in the presence of magnesium had no effect on the time constants, but increased the amplitude of the initial phase (A_1) from about 50% to 75% (Table 1). The final extent of splicing is not affected by renaturation. These results are consistent with Scheme 1, in which two forms of the pre-rRNA are in slow equilibrium at 30 °C: one that is predisposed toward self-splicing and another that must pass through an additional rate-determining transformation. Renaturation of the RNA would be expected to alter the fraction of molecules in each population at the start of the assay, but not to change the rate of isomerization at 30 °C.

Rate of Isomerization. The time constants and amplitudes obtained from eq 1 represent a combination of microscopic rate constants (eq 2). These data do not permit exact determination of the individual rate constants defined in Scheme 1. In practice, however, the time constants λ_1 and λ_2 will be roughly equal to the rate constants of the individual steps when λ_1 is much larger than λ_2, and the amplitudes roughly proportional to the fraction of molecules in each population. Using this approximation, we obtain an upper limit for the rate of self-splicing (k_{sp}) of 2.5 min^{-1}, somewhat faster than previously reported (0.5−0.6 min^{-1}; Bass & Cech, 1984; Williamson et al., 1987). Similarly, the rate of isomerization, k_I, is estimated to be on the order of 0.02 min^{-1}.

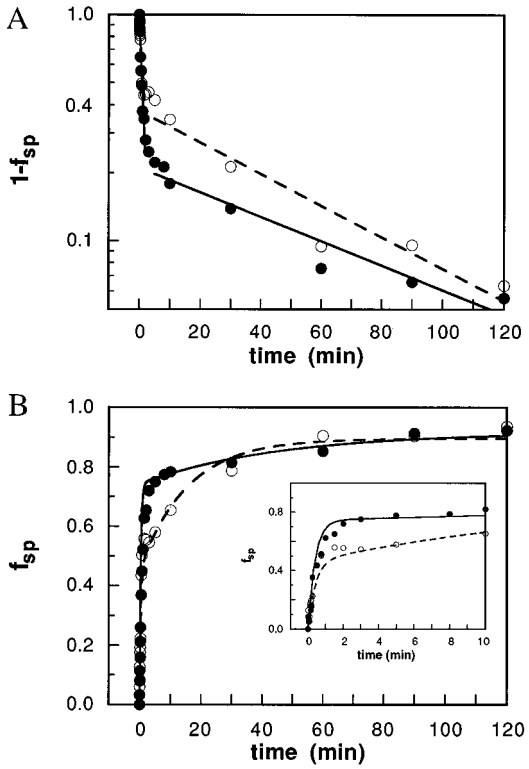

FIGURE 2: Self-splicing of wild type pre-rRNA. (A) Semilogarithmic plot of $1 - f_{sp}$ vs time at 30 °C with 0.1 mM GTP. Fraction of spliced products (f_{sp}) is based on appearance of ligated exons as described in Materials and Methods. Lines represent best linear fits to data at short (0−2 min) and long (10−120 min) times. (B) Representative plot of fraction of spliced products (f_{sp}) vs time. Data points are compared to theoretical curve from eq 1 using average parameters listed in Table 1. The data are the same as in part A. Inset: Expansion of first 10 min of reaction course. Solid circle and solid line, pre-rRNA was renatured prior to start of reaction; open circle and dashed line, pre-rRNA was not renatured.

Scheme 1

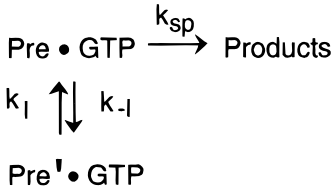

Slow- and Fast-Splicing Pre-rRNA Populations Are Conformationally Related. The independent reaction of two nonequilibrating pre-rRNA populations is also described by an equation with two exponential terms. Consequently, the shape of the progress curves alone does not distinguish between this mechanism and Scheme 1. One problem is that a nonconsecutive reaction mechanism implies the existence of two catalytic structures, for which there is no evidence at the present time. Consequently, we wished to determine whether the slow-splicing pre-rRNA can be converted to the active form, as implied by Scheme 1.

The ability of the slow-splicing population to be activated by a second renaturation treatment was tested using an approach similar to that used for longer *Tetrahymena* pre-rRNA transcripts (Woodson & Emerick, 1993). Standard self-splicing reactions were quenched with addition of EDTA after 5 min, at which time the more reactive population of

Table 1: Rate Constants and Amplitudes for Self-Splicing Reactions

RNA[a]	±95 °C[b]	A_1[c]	λ_1 (min^{-1})[c]	A_2[c]	λ_2 (min^{-1})[c]
wt	+	0.62 ± 0.01	2.5 ± 1.1	0.20 ± 0.02	0.02 ± 0.01
	−	0.38 ± 0.04	2.6 ± 0.8	0.35 ± 0.09	0.09 ± 0.08
C-6G	+	0.28 ± 0.07	2.5 ± 1.4	0.55 ± 0.17	0.14 ± 0.13
	−	0.13 ± 0.03	2.4 ± 0.7	0.36 ± 0.03	0.20 ± 0.03
Gi27C	+	0.46 ± 0.08	2.4 ± 1.2	0.28 ± 0.04	0.12 ± 0.09
	−	0.31 ± 0.16	2.5 ± 1.8	0.46 ± 0.02	0.13 ± 0.12
C-6G;Gi27C	+	0.62 ± 0.06	1.7 ± 0.3	−[d]	−
	−	0.20 ± 0.05	3.6 ± 1.2	0.53 ± 0.02	0.22 ± 0.11
Gi27C	+	0.33 ± 0.05	1.4 ± 0.4	0.30 ± 0.03	0.02 ± 0.001
	−	0.16 ± 0.08	2.1 ± 0.3	0.39 ± 0.08	0.01 ± 0.006
C-4G;Gi27C	+	0.59 ± 0.05	1.3 ± 0.1	0.26 ±0.04	0.01 ± 0.004
	−	0.15 ± 0.01	4.2 ± 0.1	0.41 ± 0.11	0.4 ± 0.3

[a] Sequence of pre-rRNA. First two rows present data for the wild type (wt); subsequent rows present data for mutations that alter the stabilities of P1 and P(−1), as diagrammed in Figure 1. [b] (+) Precursor RNA was renatured prior to splicing assay by heating to 95 °C and cooling in the presence of splicing buffer; (−) no treatment. Final conditions were 100 mM $(NH_4)_2SO_4$, 50 mM HEPES, pH 7.5, 5 mM $MgCl_2$, and 0.1 mM GTP, 30 °C. [c] Amplitudes (A_1, A_2) and first order rate constants (λ_1, λ_2) were determined from nonlinear fits to eq 1 as described in Materials and Methods. Errors are given as the standard deviation of values obtained from 2−6 independent isolations of the RNA. The error in parameters for individual fits is typically lower than that shown. [d] Reaction curves could be fit by a single exponential in some trials.

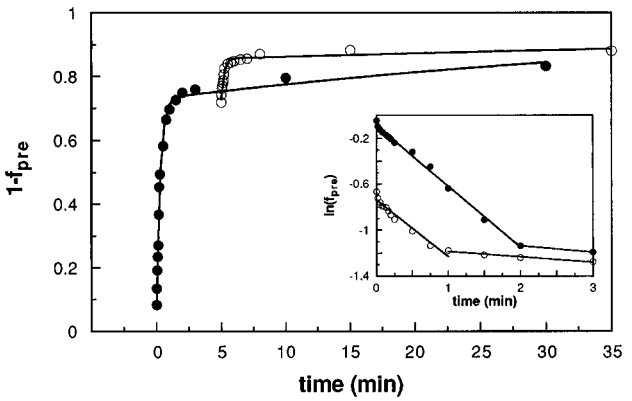

FIGURE 3: Second burst of activity following renaturation of slow-splicing RNA. Progress curves of self-splicing reactions under standard conditions as shown in Figure 2B (solid circles). After 5 min, an aliquot was removed from reaction mixture, quenched with EDTA, purified by gel filtration chromatography, and renatured by heating to 95 °C. Splicing was reinitiated with addition of GTP (open circles). Lines represent best fit to eq 1. The fraction of pre-rRNA remaining (f_{pre}) is plotted instead of f_{sp} to avoid error from loss of ligated exon RNA during gel filtration. Inset: Semilogarithmic plots of same data over initial 3 min. Times of lower curve (open circles) are relative to the time at which the reaction was restarted following renaturation.

pre-rRNA was exhausted (Figure 3). The RNA was passed over a gel filtration spin column to remove GTP and excess EDTA, and then renatured by a brief incubation at 95 °C. GTP was added back to the sample to reinitiate splicing, and the progress of the reaction monitored along with an untreated control reaction. As shown in Figure 3, renaturation resulted in a second burst of product formation similar to the first in rate and relative amplitude, consistent with redistribution of the less reactive population between slow and fast phases. It was previously demonstrated that active and inactive pre-rRNA species isolated from native gels interconvert with a rate constant of about 0.1 min^{-1} at 30 °C (Emerick & Woodson, 1994). Taken together, these results support the mechanism shown in Scheme 1, although

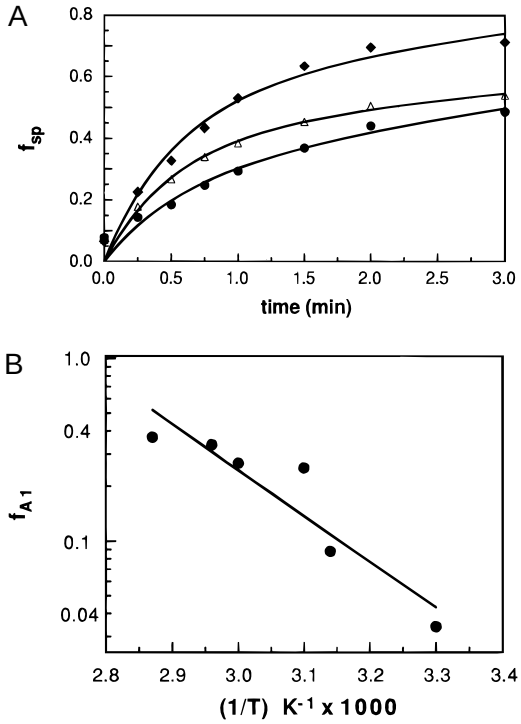

FIGURE 4: Temperature dependence of isomerization. Freshly transcribed pre-rRNA was incubated at temperatures from 30 to 95 °C for 2 min in splicing buffer, then re-equilibrated at 30 °C immediately before addition of GTP. (A) Representative fits of f_{sp} to eq 1, where λ_1 = 2.5 min^{-1} and λ_2 = 0.2 min^{-1}. RNA was preincubated at 35 °C (circles), 45 °C (triangles), and 75 °C (diamonds). (B) Arrhenius plot of the fraction of RNA in the initial rapid phase (f_{A1}) vs inverse temperature of preincubation (1/T). f_{A1} was determined from data like that shown in (A). Line is least-squares fit to data in the linear range (30−75 °C) and corresponds to an estimated activation energy of 12 kcal mol^{-1}.

they do not rule out the existence of two catalytically active forms that react independently.

Isomerization of Precursor RNA at Varying Temperatures. The change in activity of the wild type precursor upon renaturation at 95 °C suggested that the kinetic barrier to interconversion of the precursor isomers is temperature dependent. According to our working model, the amplitude of the initial phase (A_1) should increase with time as less reactive precursors refold to form the more reactive species. Self-splicing reactions were carried out at 30 °C with newly transcribed pre-rRNA that had not been renatured, under conditions in which the amount of the active species is very low. Before addition of GTP, samples were preincubated for 2 min at temperatures from 30 to 95 °C, then re-equilibrated to 30 °C. The amplitude of the initial burst was determined from fits to eq 1 in which the values of λ_1 and λ_2 were fixed (Figure 4A). At temperatures up to 75 °C, the size of the burst varies with the time of preincubation. Therefore, the fraction of reactive RNA at 2 min corresponds to the rate of interconversion. As shown in Figure 4B, a semilogarithmic plot of A_1 versus inverse temperature yields an activation energy of 12 kcal mol^{-1}. This value is very similar to the activation energy for conversion of inactive to active pre-rRNA species by native gel electrophoresis (Emerick & Woodson, 1994), but is much lower than expected for opening of RNA duplexes (Crothers et al., 1974; Freier et al., 1986).

Intermolecular Splicing. Intermolecular or trans splicing was used to further test the possibility that exchange between P(−1) and P1 is the basis for the biexponential kinetics.

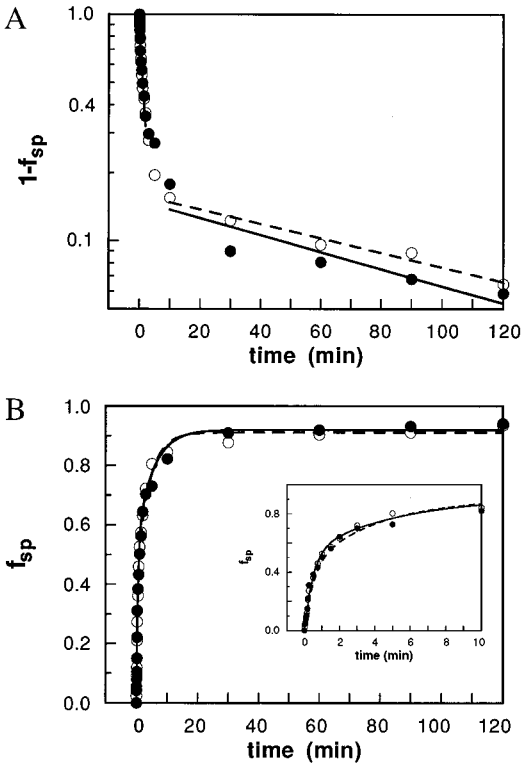

FIGURE 5: Intermolecular splicing of wild type pre-rRNA. (A) Semilogarithmic plot of $1 - f_{sp}$ vs time for representative data set at 30 °C in the absence of GTP and the presence of 70 μM 5′ exon RNA substrate, $^{5'}$rGGCUCUCU. Fraction of spliced products (f_{sp}) is based on appearance of oligonucleotide-3′ exon RNA. Fits to data at short (0−2 min) and long (10−120 min) times as in Figure 2. (B) Fraction of spliced products (f_{sp}) vs time relative to curve generated from eq 1, using parameters listed in Table 2. Inset: Expansion of first 10 min of reaction course. Symbols as in Figure 2.

Ligation of an oligonucleotide that mimics the 5′ exon to the normal 3′ exon depends on the availability of the guide sequence and activation of the 3′ splice site (Inoue et al., 1985). In very short *Tetrahymena* precursor RNAs, the relative rates of intra- and intermolecular splicing reflect the equilibrium between P(−1) and P1 (Woodson & Cech, 1991).

Trans-splicing reactions were carried out in the absence of GTP and with 70 μM oligonucleotide substrate. This concentration is sufficient to saturate the reaction rate, as determined from splicing reactions in which the substrate concentration was varied from 0.4 to 100 μM (data not shown). Progress curves for trans-splicing are also strongly biphasic (Figure 5A), and the data were treated as described above (Figure 5B and Table 2). Although the initial rate of trans-splicing ($\lambda_1 = 2$ min^{-1}) is very similar to that of cis-splicing, the amplitude of the burst (47%) is slightly reduced. Unlike cis-splicing, trans-splicing activity of the wild type precursor was not altered by renaturation of the pre-rRNA (Table 2), in agreement with earlier work (Emerick & Woodson, 1993). This suggests that the primary defect in the less reactive species is recognition of the 5′ splice site.

Comparison of Wild Type and Mutant Precursors. In order to test whether the two kinetic phases were related to the formation of alternative secondary structures near the 5′ splice site, mutations that destabilized either P1 or P(−1) were introduced in the IGS and 5′ exon as shown in Figure 1. The reaction profiles of the mutated pre-rRNAs were also biphasic, and curves were fit to eq 1. The initial rates of

Table 2: Rate Constants and Amplitudes for Intermolecular Splicing Reactions

RNA[a]	±95 °C[b]	A_1[c]	λ_1 (min^{-1})[c]	A_2[c]	λ_2 (min^{-1})[c]
wt	+	0.47 ± 0.03	2.0 ± 0.2	0.35 ± 0.05	0.19 ± 0.03
	−	0.32 ± 0.01	2.0 ± 0.3	0.37 ± 0.01	0.25 ± 0.02
C-6G	+	0.25 ± 0.07	3.5 ± 1.8	0.72 ± 0.17	0.15 ± 0.14
	−	0.41 ± 0.02	1.0 ± 0.4	0.47 ± 0.07	0.02 ± 0.01
Gi27C	+	0.44 ± 0.07	4.3 ± 1.3	0.46 ± 0.01	0.12 ± 0.10
	−	0.26 ± 0.01	7.5 ± 0.6	0.61 ± 0.02	0.35 ± 0.07
C-6G;Gi27C	+	0.39 ± 0.05	3.5 ± 0.8	0.51 ± 0.06	0.26 ± 0.01
	−	0.20 ± 0.08	4.3 ± 2.1	0.67 ± 0.08	0.39 ± 0.05
Gi25C	+	0.52 ± 0.08	3.0 ± 0.7	0.39 ± 0.10	0.05 ± 0.05
	−	0.31 ± 0.08	2.9 ± 0.2	0.62 ± 0.10	0.02 ± 0.005
C-4G;Gi25C	+	0.36 ± 0.04	2.8 ± 1.0	0.54 ± 0.12	0.03 ± 0.03
	−	0.17 ± 0.05	5.5 ± 1.2	0.27 ± 0.05	0.30 ± 0.001

[a] As in Table 1. [b] Reactions carried out as in Table 1, but contained 0.5−0.7 μM precursor RNA and 70 μM $^{5'}$rGGCUCUCU and no GTP. [c] As in Table 1.

splicing (λ_1) are similar to those of the wild type within experimental uncertainty (Table 1). However, the amplitudes of the fast and slow phases correlate in a qualitative manner with the predicted relative stabilities of P1 and P(−1). The amplitude of the first phase (A_1) is reduced relative to that of the slow phase (A_2) with mutations that destabilize P1, such as Gi25C and Gi27C, particularly in the absence of renaturation. Compensatory base changes that restore P1 but destabilize P(−1), such as C-4G;Gi25C or C-6G;Gi27C, result in a slightly higher value for A_1, as expected. The base change C-4G generally results in very poor splicing due to gross misfolding of the pre-rRNA (data not shown).

Trans-splicing activities of mutant precursors were also compared to the wild type, as shown in Table 2. Reactions of precursors with a base change in the IGS were carried out with oligonucleotide substrates containing a compensatory sequence change, so that the P1 pairing was maintained. As expected, mutations that disrupt the intramolecular P1 pairing (Gi27C, Gi25C) have little affect on trans-splicing activity. Double mutations that restore P1 at the expense of P(−1) C-4G;Gi25C and C-6G;Gi27C exhibit a slightly lower fraction of RNA in the initial burst compared to the wild type.

Taken together, these results are consistent with a model in which the distribution of pre-rRNA molecules between active and less active conformations is sensitive to the relative stabilities of the P1 and P(−1) hairpins. This also agrees with the interpretation that the alternative conformation primarily affects recognition of the 5′ splice site in the first step of splicing, although it could also involve changes in the intron core. The magnitude of the effects seen here, however, is smaller than for similar mutations in short precursors (Woodson & Cech, 1991), suggesting that additional interactions within the rRNA exons contribute to stabilization of the active form of the pre-rRNA.

Analysis of Pre-rRNA Conformation by Native Gel Electrophoresis. Native polyacrylamide gel electrophoresis was used to determine whether there is a correlation between alternative pre-rRNA structures and the magnitudes of the kinetic phases. As shown in Figure 6, the wild type precursor migrates in two bands in the absence of substrate. The slower migrating species (band 1) has been shown to contain precursor that primarily undergoes trans-splicing, whereas the faster form (band 4) contains pre-rRNA that is also active in cis-splicing (Emerick & Woodson, 1994). A minor third species, band 2b, also appears in lanes C-6G and Gi27C.

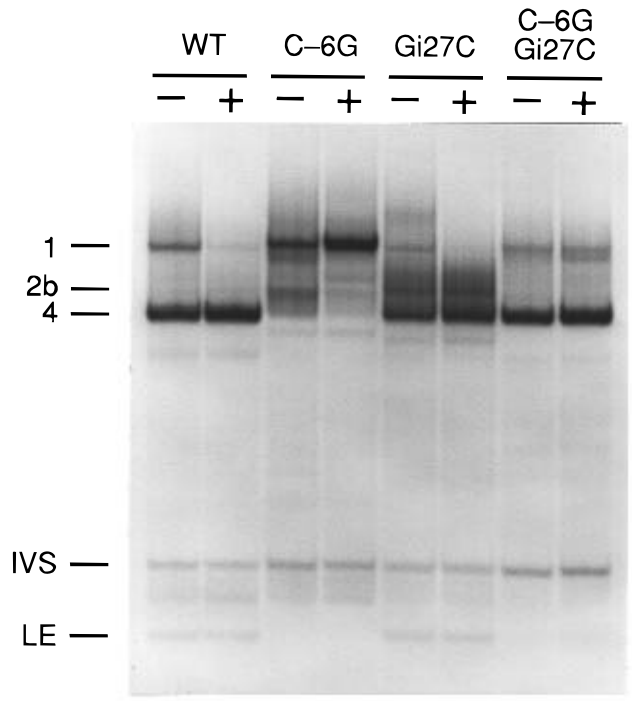

FIGURE 6: Separation of pre-rRNA conformers by native gel electrophoresis. Wild type and mutant pre-rRNAs were separated on a 6% polyacrylamide nondenaturing gel containing 10 mM $MgCl_2$. (−) RNA was not renatured; (+) RNA was renatured by heating to 95 °C before loading. Bands 1−4 correspond to pre-rRNA and have been previously characterized (Emerick & Woodson, 1994; Emerick, 1995). Band 1, partially active (trans-splicing); band 2b, partially active (rapid trans-splicing); band 4, fully active (cis- and trans-splicing); IVS, free intron; LE, ligated exon RNA.

This form of pre-rRNA is in slow exchange with band 4 and is much more reactive in trans-splicing than in cis-splicing (Emerick, 1995).

In the mutant pre-rRNAs, the distribution of radioactivity between bands 1 and 4 is altered in a manner that roughly correlates with the observed self-splicing activity in solution. In particular, the amplitude of the burst, A_1, is roughly proportional to the fraction of pre-rRNA in band 4. For example, the C-6G precursor splices poorly after renaturation ($A_1 = 0.25$) and exhibits little or no band 4 RNA in Figure 6. On the other hand, the C-6G;Gi27C precursor which splices well ($A_1 = 0.62$) primarily migrates as band 4 RNA. In some trials this precursor migrates with an anomalously slow mobility when unrenatured, suggesting that it tends to misfold during in vitro transcription. Taken together, the results from native gel electrophoresis generally support the interpretation that the kinetic phases observed in solution result from distribution of the pre-rRNA population among alternative structures, at least some of which affect 5′ splice site recognition.

Chemical Steps of Splicing Are Rapid Relative to Conformational Changes. We have previously shown that band 4 pre-rRNA undergoes a rapid shift in mobility on native gels in the presence of GTP (Emerick & Woodson, 1994). This species (band 3; Figure 7A) contains a mixture of precursor and spliced products; the proportion of product increases with time and GTP concentration (Emerick, 1995). This mobility shift is essentially complete after 10 s preincubation at 30 °C or 1 min at 4 °C. Even taking into account the time required for samples to enter the gel (30 s), we estimate the rate of the G shift to be at least 4 min^{-1} at 30 °C, equal to or greater than the initial rate of splicing

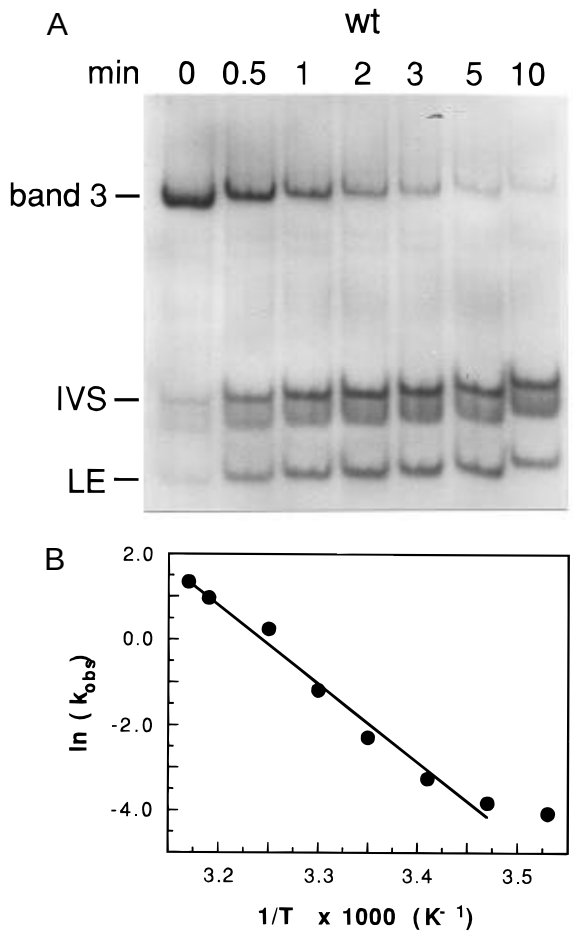

FIGURE 7: Dissociation of product complexes. (A) Wild type pre-rRNA was renatured and incubated with 0.1 mM GTP for 1 min at 30 °C (lane 0), then shifted to 40 °C, and aliquots were removed at times specified above the lanes before electrophoresis on nondenaturing 6% polyacrylamide gel. Band 3, product complex and activated pre-rRNA; IVS, free intron; LE, free ligated exon product. From denaturing gels, 85% of the pre-rRNA is spliced at the start of the assay (lane 0). (B) Semilogarithmic plot of observed rates of product dissociation (k_{obs}) from 10−42 °C vs inverse temperature (1/*T*). The slope of the best fit (15−40 °C) corresponds to an apparent activation energy of 39 kcal mol^{-1}.

Scheme 2

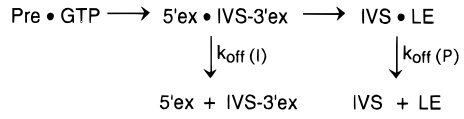

in solution. Therefore, structural and chemical transformations that follow GTP binding in self-splicing appear to be much more rapid than initial folding of the pre-rRNA, consistent with results from the multiple turnover endonuclease reaction (Herschlag & Cech, 1990).

Product Dissociation. Unlike multiple turnover systems, the rate of product release in self-splicing cannot be directly determined from reaction kinetics. However, as the product complex of the 657 nt precursor used in these experiments is readily distinguished from the free intron and ligated exon products on native gels, this approach was used to measure the rate and apparent activation energy of product dissociation, or k_{off}(P) in Scheme 2. As shown in Figure 7A, after GTP addition the product complex (band 3) disappears with time when incubated at 40 °C before loading of the sample. At the same time, bands corresponding to free intron and ligated exon RNAs increase in intensity. Dissociation rates were determined from the fraction of band 3 versus time.

Table 3: Rates of Spliced Product Dissociation[a]

temp (°C)	0.1 mM GTP wt (min^{-1})	0.5 mM GTP wt (min^{-1})	0.5 mM GTP G414A (min^{-1})[b]
10	0.019		
15	0.021		
20	0.038		
25	0.10		
30	0.31	0.55	2.8×10^{-3}
35	1.28		
40	2.64		
42	3.4		

[a] Precursor RNA was incubated in splicing buffer with 0.1 or 0.5 mM GTP and 10% glycerol. Rates determined from the fraction of dissociated product RNA vs time as measured by native gel electrophoresis. [b] Dissociation of intermediate complex was based on appearance of free intron-3′ exon RNA. Spliced products (intron and ligated exons) also appear with time but were not in included in this calculation.

Renatured pre-rRNA was preincubated with 0.1 M GTP for 1 min or 0.5 M GTP for 30 s at 30 °C to minimize the amount of unspliced precursor at the start of the assay. Association of intron and ligated exon RNAs is not detectable under these conditions (data not shown).

As shown in Table 3, the rate of product release (0.3−0.5 min^{-1}) is slower than splicing of the reactive form of the precursor (∼2 min^{-1}) at 30 °C. At 50 °C, dissociation of the ligated exons is much more rapid and is essentially complete within the time required to load samples into the gel (30 s). Rates of dissociation over the range 10−42 °C revealed an apparent Arrhenius activation energy of 36.6 kcal mol^{-1}, from which we estimate $\Delta H^{\ddagger} = E_a - RT = 36.0$ kcal mol^{-1}. This value is lower than the enthalpy for base pairing between the 5′ exon and IGS ($\Delta H^{\circ} = 60$ kcal mol^{-1}; Pyle et al., 1994) and much lower than expected if both P1 and the P10 pairing between the 3′ exon and the IGS are taken into account (about 100 kcal mol^{-1}; Freier et al., 1986). Assuming a frequency factor of *RT*/*Nh*, we estimate the activation entropy $\Delta S^{\ddagger} = 70$ eu.

Dissociation of Intermediate Complex. After the first transesterification, the 5′ exon remains noncovalently bound to the IVS-3′ exon in an intermediate complex (Scheme 2). As the first step of splicing is slower than the second step for *Tetrahymena* pre-rRNA, splicing intermediates do not accumulate under these conditions. The lack of intermediates has also been attributed to the stability of the P1 helix, which prevents premature dissociation of the 5′ exon after cleavage of the 5′ splice site (Herschlag & Cech, 1990). However, we find the rate of ligated exon release to be appreciable, even though association of the ligated exons and the intron also depends on P1. Therefore, it was of interest to determine whether the 5′ exon dissociates from the intermediate complex at a rate similar to release of the ligated exons.

Release of the 5′ exon following the first step of splicing, k_{off}(I) in Scheme 2, was measured using a precursor in which the terminal guanosine of the intron G414 was mutated to A. This base change impairs 3′ splice site recognition and leads to accumulation of 5′ exon and IVS-3′ exon RNA (Been & Perrotta, 1991). As shown in Figure 8A, the intermediate complex, which migrates as band 4 in nondenaturing gels, dissociates approximately 100-fold more slowly (0.003 min^{-1}) than the product complex at 30 °C. This is not due to slow cleavage of the 5′ splice site, since the first step of splicing is essentially complete after a 2 min preincubation with 0.5 M GTP (lanes 9 and 10 in Figure 8B). The rates of G addition are essentially the same for the wild type and G414A RNAs. The large difference in the dissociation rates of the 5′ exon (k_{off}(I)) and the ligated exons (k_{off}(P)) implies that additional interactions within the precursor specifically stabilize the intermediate relative to the final product complex and could account for the very low accumulation of splicing intermediates in the wild type pre-rRNA.

DISCUSSION

Exchange of Alternative Pre-rRNA Structures. We have investigated self-splicing of a precursor RNA that is derived from pre-rRNA sequences of *Tetrahymena* in order to establish an initial kinetic framework for the natural splicing reaction. Previous work has shown that the ribosomal RNA exons are important for intron excision (Woodson, 1992; Woodson & Emerick, 1993). In particular, the exons modulate the balance between alternative P(−1) and P1 hairpins, which in turn affects 5′ and possibly 3′ splice site activation (Woodson & Cech, 1991).

Analysis of intramolecular and intermolecular splicing reactions under conditions of high GTP concentration has revealed two kinetic phases for which the time constants differ by an order of magnitude. This outcome provides evidence for the presence of at least one additional kinetic species before transesterification with GTP, as depicted in Figure 9. A slow conformational change prior to chemistry is the most likely explanation of the data and in agreement with separation of this pre-rRNA into multiple forms on nondenaturing polyacrylamide gels (Emerick & Woodson, 1994). At early times, the observed splicing rate is dominated by splicing of correctly folded RNA; at later times, the rate of splicing at physiological temperatures is proposed to be limited by the rate of refolding an inactive structure. Under the conditions of T7 in vitro transcription, a larger fraction of the pre-rRNA reacts in the slow phase, in agreement with earlier results showing that *Tetrahymena* pre-rRNAs are trapped in an inactive form during transcription (Emerick & Woodson, 1993).

Mutations that stabilize or destabilize the P1 and P(−1) hairpins alter the amplitudes of the kinetic phases in a manner consistent with their proposed secondary structure. These mutations also alter the distribution of the pre-rRNA among active and partially active conformers on native gels. The fraction of pre-rRNA in each native gel band correlates in a qualitative way with the splicing kinetics in solution. The magnitudes of the mutational effects, while consistent, are not large. A number of interactions contribute to the stability of the pre-rRNA and may limit the effect of single base changes on splicing activity. It is also possible that base changes in P1 indirectly affect the slow phase of the reaction profiles. These methods can only detect processes that are kinetically well-resolved from the initial burst of product formation; thus we do not exclude the possibility of other rapid changes in pre-rRNA structure. In fact, native gel mobilities would suggest that there are at least three stable forms of the pre-rRNA in the absence of GTP (bands 1, 2b, and 4), suggesting that the folding pathway is more complicated than shown in Figure 9.

The slow rate of pre-rRNA isomerization at 30 °C (0.09−0.02 min^{-1}) and the large change in electrophoretic mobility are consistent with a significant conformational rearrangement. Exchange between P1 and P(−1) helices could

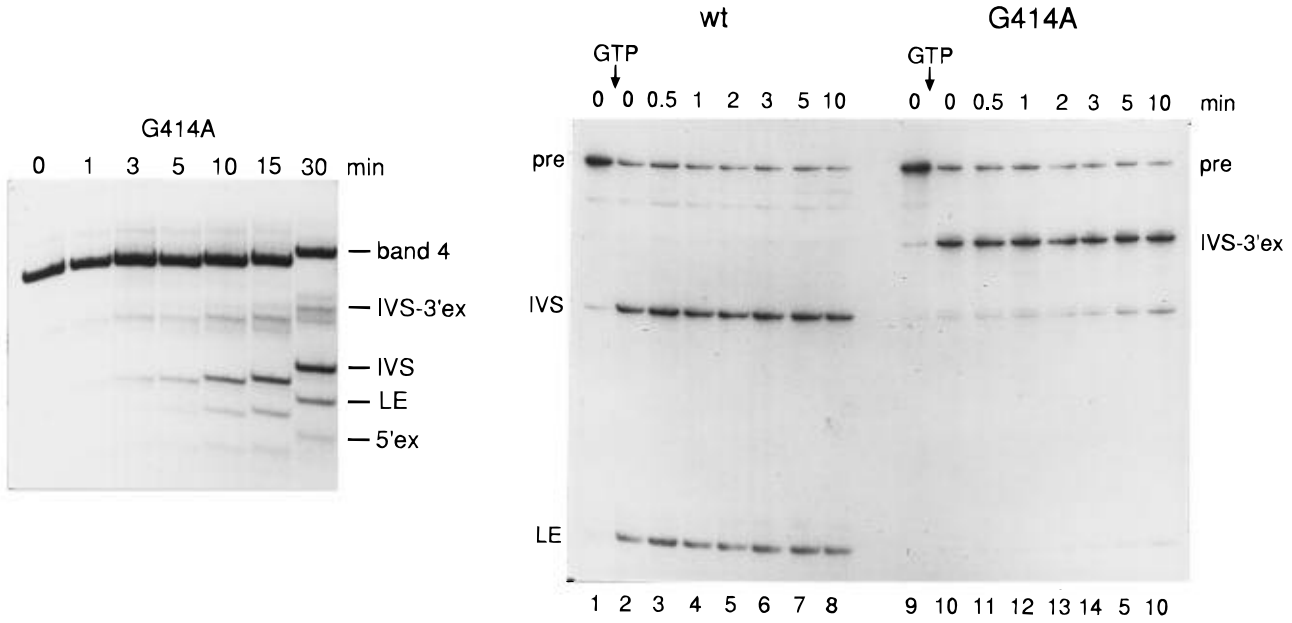

FIGURE 8: Dissociation of splicing intermediate complexes. (A) G414A pre-rRNA was renatured and incubated with 0.5 mM GTP for 2 min at 30 °C in splicing buffer (lane 0), then shifted to 30 °C, and aliquots were loaded on a 6% native gel at specified times as in Figure 7. Band 4, intermediate complex; IVS-3′ex, intron-3′ exon intermediate; IVS, intron; LE, ligated exons; 5′ex, 5′ exon. (B) 4% sequencing gel of pre-rRNA treated as in (A), showing conversion of precursor to spliced products (wt, lanes 1 and 2) or intermediates (G414A, lanes 9 and 10) during preincubation with GTP. RNAs labeled as above.

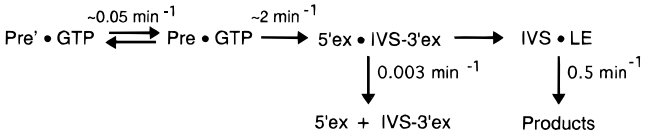

FIGURE 9: Kinetic model for self-splicing of *Tetrahymena* pre-rRNA. The rate of refolding of inactive pre′-rRNA is based on the slow phase of self-splicing (0.02 min^{-1} or 0.09 min^{-1}, with or without renaturation respectively) and is similar to the value obtained from native gel assays (0.1 min^{-1}; Emerick & Woodson, 1994). The apparent activation energy for this process is 10−12 kcal mol^{-1}. In the initial burst, the rate of splicing is on the order of 2−3 min^{-1}, significantly faster than refolding of inactive pre-rRNA. For the wild type precursor, the second step of splicing is not rate determining. Dissociation of the 5′ exon following G-addition is based on dissociation of the G414A intermediate complex; the rate constant of ligated exon dissociation is derived from the wild type product complex. The apparent activation energy for spliced product dissociation is 39 kcal mol^{-1}.

conceivably induce a large change in the hydrodynamic radius of the pre-rRNA. The difference in mobility could also arise from a greater degree of compactness or "tertiary" structure in the reactive pre-rRNA (band 4). It is possible that the slow rate of exchange reflects slow formation of tertiary contacts within the intron core. Zarrinkar and Williamson (1994) estimated the folding rate for long-range helices (P3−P7) in the intron core to be 0.7 min^{-1} at 37 °C. We find it more likely that isomerization is slow because it also requires at least partial unfolding of the pre-rRNA (Thirumalai & Woodson, 1996). This could include exchange between P(−1) and P1, but may also involve rearrangement of inappropriate contacts in the intron core. In fact, temperatures used for this study (45−95 °C) are high enough to permit renaturation of the intron RNA (Walstrum & Uhlenbeck, 1990; Celander & Cech, 1991; Banerjee et al., 1993). The low apparent activation energy for conversion of inactive and active structures (12 kcal mol^{-1}) is more consistent with disruption of tertiary interactions than with opening of P(−1) helix as the rate-determining process and is in agreement with our earlier results from native gel assays (Emerick & Woodson, 1994). At the same time, interconversion of P(−1) and P1 may be facilitated by a strand-exchange mechanism similar to branch migration. Further experiments are required to test these possibilities.

Conformational Change after the First Step of Splicing. Once the active pre-rRNA has been formed, it reacts rapidly with bound GTP to yield spliced products. Exchange between the G added to the 5′ end of the intron in the first step and G414 implies at least one additional conformational step between cleavage of the 5′ splice site and exon ligation. This rearrangement must be at least as fast as the overall rate of splicing (∼2.5 min^{-1}), since intermediate products are not observed. Moreover, the rates of intermolecular exon ligation are comparable to the rates of cis-splicing. Finally, the rates of G transesterification with wild type and G414A pre-rRNAs, in which 3′ splice site recognition is impaired, are nearly identical (data not shown), further evidence that activation of the 3′ splice site is independent of 5′ splice site cleavage and does not determine the overall rate of splicing for the wild type pre-rRNA.

Dissociation of Product Complexes. Release of oligonucleotide substrates limits the rate of intermolecular enzymatic reactions of the *Tetrahymena* intron (Herschlag & Cech, 1990). For pre-rRNA, product dissociation measured by a native gel assay is slower than the rate of self-splicing at 30 °C (0.5 min^{-1} vs 2.5 min^{-1}). Mutations that destabilize P1 increase the rate of ligated exon dissociation as expected (J. Pan and S. Woodson, unpublished), suggesting that product release does depend on the P1 duplex. However, the product release after splicing is much slower than unpairing of a duplex that mimics P1 (approximately 50 min^{-1} at 30 °C from optical melting curves; Pyle et al., 1994). Either our native gel assay underestimates the spliced product dissociation rates by 100-fold, or tertiary interactions between P1 and the intron core as well as interactions within the extended rRNA exons retard product dissociation.

The Intermediate Complex Is More Stable Than the Product Complex. Dissociation of the 5′ exon after the first

step of splicing is 100-fold slower than release of ligated exons, despite the potential for additional base pairs between the 3′ exon and the IGS in the latter. This important observation demonstrates that non-base pairing interactions stabilize the intermediate complex relative to the product complex. One possibility is that P1 remains docked in the active site after the first step of splicing (Bevilacqua et al., 1996), but tends to become undocked following ligation of the 5′ and 3′ exons. Docking interactions stabilize the P1 helix by about 3 kcal mol^{-1} at 30 °C (Li et al., 1996), roughly corresponding to a 100-fold difference in dissociation rates. For oligonucleotide substrates, undocking of the P1 helix is accompanied by an unfavorable entropy of activation (Li et al., 1996). Our preliminary data also suggest that release of the 5′ exon is entropically less favorable than release of the ligated exons but that the activation energies for the two events are nearly the same.

On the other hand, 5′ exon dissociation (0.003 min^{-1}) and even product release (0.5 min^{-1}) for splicing are much slower than undocking of P1, which has been estimated to be 8 min^{-1} at 25 °C from fluorescence experiments (Li et al., 1996) and 8×10^4 min^{-1} based on miscleavage rates at 50 °C (Herschlag, 1992) for oligonucleotide substrates bound to the *Tetrahymena* ribozyme. Therefore, docking of P1 into the active site does not appear sufficient to account for the association of the 5′ exon, and we again conclude that other interactions within the intron or rRNA exons contribute to the overall stability of the splicing complex. It is possible that reaction conditions (e.g., NaCl vs $(NH_4)_2SO_4$) account for some differences in results obtained with the *Tetrahymena* ribozyme and pre-rRNA. However, 5′ exon oligonucleotide analogs have been recently found to dissociate more slowly than ligated exon analogs from a ribozyme that terminates in G414 (Mei & Herschlag, 1996).

Conclusion. In protein enzymes, reaction turnover is often coupled to conformational changes. This also appears to be the case for RNA catalysts. For the *Tetrahymena* pre-rRNA, the thermodynamic equilibrium is delicately tipped in favor of the structures that self-splice. Over the course of the splicing reaction, a sequential exchange of interactions between the intron core and nucleotides at the splice sites ensures coordinate recognition of 5′ and 3′ splice sites and correct exon ligation. Finally, destabilization of the product complex relative to the intermediate complex promotes release of the excised intron. This is biologically important, in that prolonged association of the intron with the ligated exons could interfere with function of the mature transcript and even promote the reverse splicing reaction.

REFERENCES

Banerjee, A. R., Jaeger, J. A., & Turner, D. H. (1993) *Biochemistry 32*, 153−163.

Bass, B., & Cech, T. R. (1984) *Nature 308*, 820−826.

Been, M. D., & Cech, T. R. (1986) *Cell 47*, 207−216.

Been, M. D., & Perrotta, A. T. (1991) *Science 252*, 434−437.

Been, M. D., Perrotta, A. T., & Rosenstein, S. P. (1992) *Biochemistry 31*, 11843−11952.

Bevilacqua, P. C., Kierzek, R., Johnson, K. A., & Turner, D. H. (1992) *Science 258*, 1355−1358.

Bevilacqua, P. C., Sugimoto, N., & Turner, D. H. (1996) *Biochemistry 35*, 648−658.

Burke, J. M. (1988) *Gene 73*, 273−294.

Cantor, C. R., & Schimmel, P. R. (1980) *Biophysical Chemistry*, pp 889−891, W. H. Freeman, San Francisco.

Cech, T. R., & Bass, B. L. (1986) *Annu. Rev. Biochem. 55*, 599−629.

Cech, T. R., Herschlag, D., Piccirilli, J. A., & Pyle, A. M. (1992) *J. Biol. Chem. 267*, 17479−17482.

Celander, D. W., & Cech, T. R. (1991) *Science 251*, 401−407.

Chebli, K., Gattoni, R., Schmitt, P., Hildwein, G., & Stevenin, J. (1989) *Mol. Cell. Biol. 9*, 4852−4861.

Crothers, D. M., Cole, P. E., Hilbers, C. W., & Shulman, R. G. (1974) *J. Mol. Biol. 87*, 63−88.

Dammel, C. S., & Noller, H. F. (1993) *Genes Dev. 5*, 2521−2532.

D'Orval, B. C., Carafa, Y. D., Sirand-Pugnet, P., Gallego, M., Brody, E., & Marie, J. (1991) *Science 252*, 1823−1828.

Emerick, V. L. (1995) Ph.D. Thesis, University of Maryland, College Park.

Emerick, V. L., & Woodson, S. A. (1993) *Biochemistry 32*, 14062−14067.

Emerick, V. L., & Woodson, S. A. (1994) *Proc. Natl. Acad. Sci. U.S.A. 91*, 9675−9679.

Eng, F. J., & Warner, J. R. (1991) *Cell 65*, 797−804.

Fedor, M. J., & Uhlenbeck, O. C. (1990) *Proc. Natl. Acad. Sci. U.S.A. 87*, 1668−1672.

Fortner, D. M., Troy, R. G., & Brow, D. A. (1994) *Genes Dev. 8*, 221−223.

Freier, S. M., Kierzek, R., Caruthers, M. H., Neilson, T., & Turner, D. H. (1986) *Proc. Natl. Acad. Sci. U.S.A. 83*, 9373−9377.

Golden, B. L., & Cech, T. R. (1996) *Biochemistry 35*, 3754−3763.

Herschlag, D. (1992) *Biochemistry 31*, 1386−1399.

Herschlag, D., & Cech, T. R. (1990) *Biochemistry 29*, 10159−10171.

Herschlag, D., & Khosla, M. (1994) *Biochemistry 33*, 5291−5297.

Inoue, T., Sullivan, F. X., & Cech, T. R. (1985) *Cell 43*, 431−437.

Kunkel, T. A., Roberts, J. D., & Zakour, R. A. (1987) *Methods. Enzymol. 154*, 367−382.

Li, Y., Bevilacqua, P. C., Mathews, D., & Turner, D. H. (1996) *Biochemistry* (in press).

Libri, D., Piseri, A., & Fiszman, M. Y. (1991) *Science 252*, 1842−1845.

McConnell, T. S., & Cech, T. R. (1995) *Biochemistry 34*, 4056−4067.

McConnell, T. S., Cech, T. R., & Herschlag, D. (1993) *Proc. Natl. Acad. Sci. U.S.A. 90*, 8362−8366.

Mei, R., & Herschlag, D. (1996) *Biochemistry 35*, 5796−5809.

Olender, D. L., Zurawski, G., & Yanofsky, C. (1979) *Proc. Natl. Acad. Sci. U.S.A. 76*, 5524−5528.

Pyle, A. M., McSwiggen, J. A., & Cech, T. R. (1990) *Proc. Natl. Acad. Sci. U.S.A. 87*, 8187−8191.

Pyle, A. M., Murphy, F. L., & Cech, T. R. (1992) *Nature 358*, 123−128.

Pyle, A. M., Moran, S., Strobel, S. A., Chapman, T., Turner, D. H., & Cech, T. R. (1994) *Biochemistry 33*, 13856−13863.

Séraphin, B., Simon, M., & Faye, G. (1988) *EMBO J. 7*, 1455−1464.

Strobel, S. A., Cech, T. R., Usman, N., & Beigelman, L. (1995) *Science 267*, 675−678.

Szabó, Z. G. (1969) in *Comprehensive Chemical Kinetics* (Bamford, C. H., & Tipper, C. F. H., Eds.) Vol. 2, pp 24−26, Elsevier, Amsterdam.

Thirumalai, D., & Woodson, S. A. (1996) *Acc. Chem. Res.* (in press).

Walstrum, S., & Uhlenbeck, O. C. (1990) *Biochemistry 29*, 10573−10576.

Williamson, C. L., Tierney, W. M., Keiker, B. J., & Burke, J. M. (1987) *J. Biol. Chem. 262*, 14672−14682.

Woodson, S. A. (1992) *Nucleic Acids Res. 20*, 4027−4032.

Woodson, S. A., & Cech, T. R. (1989) *Cell 57*, 335−345.

Woodson, S. A., & Cech, T. R. (1991) *Biochemistry 30*, 2042−2050.

Woodson, S. A., & Emerick, V. L. (1993) *Mol. Cell. Biol. 13*, 1137−1145.

Zarrinkar, P. P., & Williamson, J. R. (1994) *Science 265*, 918−924.

Zaug, A. J., & Cech, T. R. (1986) *Science 231*, 470−475.

Zavanelli, M. I., & Ares, M, Jr. (1991) *Genes Dev. 5*, 660−670.

BI960865I